Vacuum 155 (2018) 682–688

Contents lists available at ScienceDirect

Vacuum

journal homepage: www.elsevier.com/locate/vacuum

Nanocubic magnesium oxide: Towards hydrazine sensing

Rizwan Wahab[a,*], Naushad Ahmad[b], Manawwer Alam[b], Anees A. Ansari[c]

[a] Zoology Department, College of Science King Saud University, Riyadh 11451, Saudi Arabia
[b] Department of Chemistry, College of Science, King Saud University, P.O. Box 2455, Riyadh, Saudi Arabia
[c] King Abdullah Institute for Nanotechnology, King Saud University, P.O. Box 2455, Riyadh 11451, Saudi Arabia

ARTICLE INFO

Keywords:
Nanosensors
Magnesium oxide
Hydrazine
FTIR and TGA

ABSTRACT

The magnesium oxide (MgO), which is a thermodynamically stable material, has great property of sensing in liquid medium. To keep this point, the present work was designed to show the preparation of cubic shaped MgO nanoparticles (CNMgO) by wet chemical reaction and their sensing purposes in presence of hydrazine solution. The processed material was characterized with X-ray diffraction pattern (XRD) to evaluate their crystalline property, whereas the morphology of nanostructure was examined with transmission electron microscopy (TEM), reveals the size of obtained material is in the range of ~100 nm with cubic form. The chemical functional changes were analyzed via the FTIR spectroscopy; authenticate the conversion of hydroxide in to metal oxide. The Thermo-gravimetric analysis (TGA) was obtained the phase transition of prepared and annealed MgO was obtained at 350–400 °C temperature. The oxidation and reduction potential of CNMgO in hydrazine solution was analyzed from lower to higher (from 0.1 to 1mL/100 mL PBS, 1 mL to 5 mL/100 mL PBS, 10 μL to 100 μL/100 mL PBS) concentration via cyclic voltammetry (CV). On the basis of the results and their observations, we have also described the possible pictorial mechanism of sensing of hydrazine in presence of prepared CNMgO.

1. Introduction

The industrial compound Hydrazine (N_2H_4), which behaves like ammonia, has wide applications in various industrial arenas such as treatment for boiler water or oxygen scavenger [1], fuel cells [2], rocket propellants [3], plastic foaming, polymerization [4], crosslinking agents, dyes [5,6], blowing agent [7], photographic chemicals etc [8]. Including this, hydrazine has larger applications in pharmaceutical for instance it acts as anti-tubercular drug [9], anti-cancer [10], anti-depression [11], anti-fungal [12], antiviral, pesticides etc [13]. Although, it has various applications of hydrazine, but it can cause the irritation, corrosion and are sensitive for respiration, damage human's liver, kidney and brain [14]. As per the Environmental Protection Agency (EPA), hydrazine is neurotoxin in nature and has been classified as human carcinogen [15]. Hence it's its urgent need to develop an alternative sensitive method, which should be economical, effective and highly desirable for to trace and detect the hydrazine amount [16]. Towards this area, till to date various methods have been developed for the determination of hydrazine such as chromatography, fluorescence, spectrophotometry, chemiluminescence etc [17–19]. The recent advancement in area of nanoscience and nanotechnology, which is based on nanostructures (nanoparticle, nanotubes, nanocubes, nanorods, nanowires, tetrapods etc), facilitates to detect the hazardous compounds via electrochemical studies due to their strong, effective physico-chemical, electrical, magnetic, luminescent and catalytic properties [20–25]. These unique properties of nanomaterials provide faster, sensitive and economical detection ways for various chemical and biochemical substances. Many works has been done towards the development of amperemetric, voltammetric and electrochemical sensors. Over various types of sensors, hydrazine based electrochemical sensors, which has low cost, good accessibility, selectivity, and high sensitivity and has much attention due to their applicability in various areas [26–28].

Among various metal oxides, MgO is one of the most important functional materials due to their own merits and its diversity in terms of morphologies, properties in various applications [29–31]. These versatile properties of MgO provides an opportunity to recognize itself as one of the most multifunctional materials; therefore it can be used many ways such as in hydrogen storage [32], chemical and biological sensors [33], solar cells and diodes [34], electroluminescence devices [35], photonic crystal devices photocatalyst [36], ultraviolet lasers [37], photo-detectors, etc [38]. Over various applications, the utilization of MgO nanostructures as sensor-electrode received a considerable attention and interest recently due to its high surface area, smaller in size, high thermal stability, greater catalytic properties, and high sensitivity, better performance allows rapid analysis for device fabrication

* Corresponding author. College of Science, Department of Zoology, P.O. Box 2455, King Saud University, Riyadh 11451, Saudi Arabia.
E-mail addresses: rwahab@ksu.edu.sa, rwahab05@gmail.com (R. Wahab).

https://doi.org/10.1016/j.vacuum.2018.06.026
Received 13 April 2018; Received in revised form 4 June 2018; Accepted 8 June 2018
Available online 13 June 2018
0042-207X/

in the form of an electrochemical sensors/biosensors or biochips [39,40].

In the present manuscript, a facile and very rapid method has been introduced for the synthesis of cubic nanomagnesium oxide (CNMgO) via solution process. The prepared CNMgO have been characterized in detail in terms of their physicochemical parameters such as the crystalline property of the prepared CNMgO was assessed via XRD, whereas the morphological analysis of CNMgO was performed via TEM. The chemical finger print of the prepared nanomaterial was assessed via room temperature FTIR spectroscopy. In addition to theses the thermal efficiency of the prepared material was analyzed via TGA and Derivative thermo-gravimetric (DTG). The prepared nanostructures efficiently were utilized as effective electron mediators for the fabrication of highly sensitive hydrazine chemical sensor. The fabricated hydrazine sensor based on MgONPs exhibits a good electrocatalytic activity towards electrochemical oxidation of hydrazine analyzed via the cyclic voltammetry (CV) detection at low, medium and high range of hydrazine concentration. To the best of our knowledge, this is the first report which demonstrates the utilization of cubic shaped nanomagnesium oxide nanoparticles for the fabrication of efficient hydrazine chemical sensor. By this work, it could be concluded that simply synthesized MgONPs can be used as efficient electron mediators for the fabrication of effective hydrazine chemical sensors.

2. Materials and methods

2.1. Experimental

The synthesis of MgO was carried out by using soft chemical and hydrolytic process. For the formation of nanostructures, the entire chemicals were purchased from Aldrich chemical corporation, U.S.A and utilized as received. In a typical chemical reaction for the synthesis of MgO nanoparticles, 3×10^{-2} M of $Mg(NO)_3.2H_2O$ and alkali sodium hydroxide (NaOH, 0.3 M) were dissolved in a 100 mL deionized water to form white colored solution under continuous stirring (~30 min). The resultant solution was refluxed at 90 °C for 6 h in a refluxing pot. The reaction was monitored with noting changes in pH value from 9.5 till neutral pH (7.0). The white precipitate was observed in the refluxing pot, filtered with distilled water, solvent methanol (MeOH), ethanol (EtOH) and acetone to remove the byproducts and ionic impurities in the refluxing pot. After the completion of washing, the content powder was dried in an oven for overnight at 60 °C.The resultant white powder was then calcined at 250 °C in air with a heating rate of 5 °C/min in an ambient air for 1 h (h) and the white powder was used for sensor fabrication.

2.2. Characterization

2.2.1. Crystalline, morphological and compositional measurement

The crystalline property of chemically prepared as grown and annealed powder samples were analyzed via XRD (PANalytical X′ Pert X-ray diffractometer) with a scintillation detector in reflection mode ($Cu_{K\alpha}$ radiation (λ = 1.54184 Å). The analysis was performed from 10 to -85° at scan speed of 4°/min at an accelerating voltage of 40 kV and current was 40 mA. The morphological studies of the synthesized and annealed powder were carried out by using TEM (JEOL JEM, 2010; Hitachi Japan) working with an acceleration voltage of 200 kV. For the TEM measurement of grown and annealed MgO nanostructures, the powder was ultrasonically dispersed in an ethanol solvent for 10 min and placed a droplet of MgO nanostructures the suspension on a copper grid (~400 mesh) and dried at room temperature. The chemical bonding or functional behaviors of synthesized and annealed nanostructures were analyzed with the help of FTIR spectroscopy (FTIR, Perkin Elmer's GX spectrophotometer) in the range of 4000–400 cm^{-1} with using KBr pellets.

2.2.2. Electrochemical measurements

The Electrochemical measurements were carried out on Autolab Potentiostat/galvanostat, PGSTAT 204-FRA32 control with NOVA software (Metrohom Autolab B.V.Kanaalweg 29-G, 3526 KM Utrecht, The Netherlands) in three electrode system. The working electrode was MgO modified glassy carbon electrode, platinum (pt) work as a counter whereas Ag/AgCl used as a reference electrode. Prior to coat the slurry of prepared materials (70% MgO (4.9 mg), 30% (2.1 mg) ethyl cellulose in 200 µL PBS) on the surface of Glassy carbon electrode (GCE), it was polished with polishing cloth, followed by multiple washing with distilled water (DW) thoroughly. Finally, a certain amount (~25–30 µL) of viscous slurry prepared materials was casted on the electrode surface which was then dried at 60 °C for 2 h to get a homogenous and dried layer over the carbon electrode surface. Phosphate buffer solution (PBS, pH = 7.4) was used as a background media. The prepared PBS (pH 7.2) was purged with nitrogen (N_2) gas for 10 min prior to all the electrochemical experiments. PBS sensor with hydrazine was used as an electrolyte. A wide concentration range of hydrazine (concentration from 0.1, to 1 mL/100 mL PBS, 1 mL to 5 mL/100 mL PBS, 10 µL to 100µL/100 mL PBS) was used to determine the sensing characteristics. The current response was measured from −0.2 to +2.0 V. For studying the electrical response at various concentrations, run with the scan rate 100 mV/s with or without hydrazine in 10 mL PBS.

3. Results and discussion

3.1. X-ray diffraction pattern

The XRD pattern describes the crystalline properties, particle size, phases of the prepared nanostructures. Fig. 1a depicts the XRD pattern of as grown MgO nanostructures, whereas Fig. 1b shows the diffraction pattern of annealed sample at 250 °C temperature. From the obtained graph its shows that various peaks were observed in the spectrum. The peak position at (14.51°), (20.02), (24.50), (28.31), (31.23), (33.95), (35.79), (47.04), (56.15), (62.37), (66.13), (67.57), (68.82), (72.18), (76.55), and (81.03°), these peaks corresponds to Mg peak as can be seen in the JCPDS cards (01–1141). Fig. 1b shows the sample annealed at 250 °C in air for 1 h, as the temperature/annealing increases various crystalline peaks were observed in the spectrum. The intensity of MgO peaks can be seen and confirm from the JCPDS cards (04–0829, 27–0759).

3.2. Morphological characterization (TEM results)

The structural elucidation of as processed and annealed magnesium structures were observed via TEM. It can be seen clearly from Fig. 2a that the nanostructures aspects like to cubic shaped particles. From the obtained data, the average size of the as grown nanostructures is about

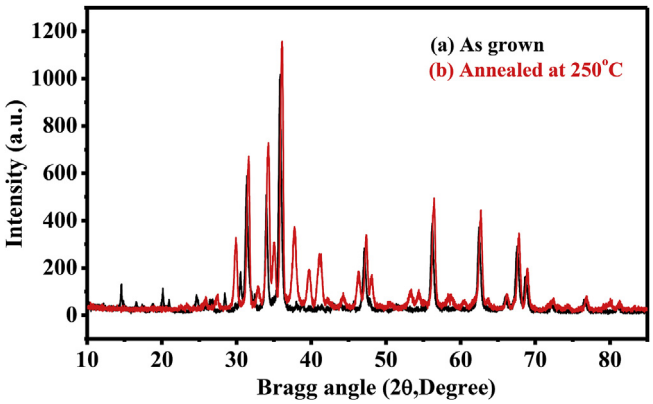

Fig. 1. The X-ray diffraction pattern of prepared powder of magnesium oxide of grown (a) and annealed at 250 °C (b) temperature for an hour.

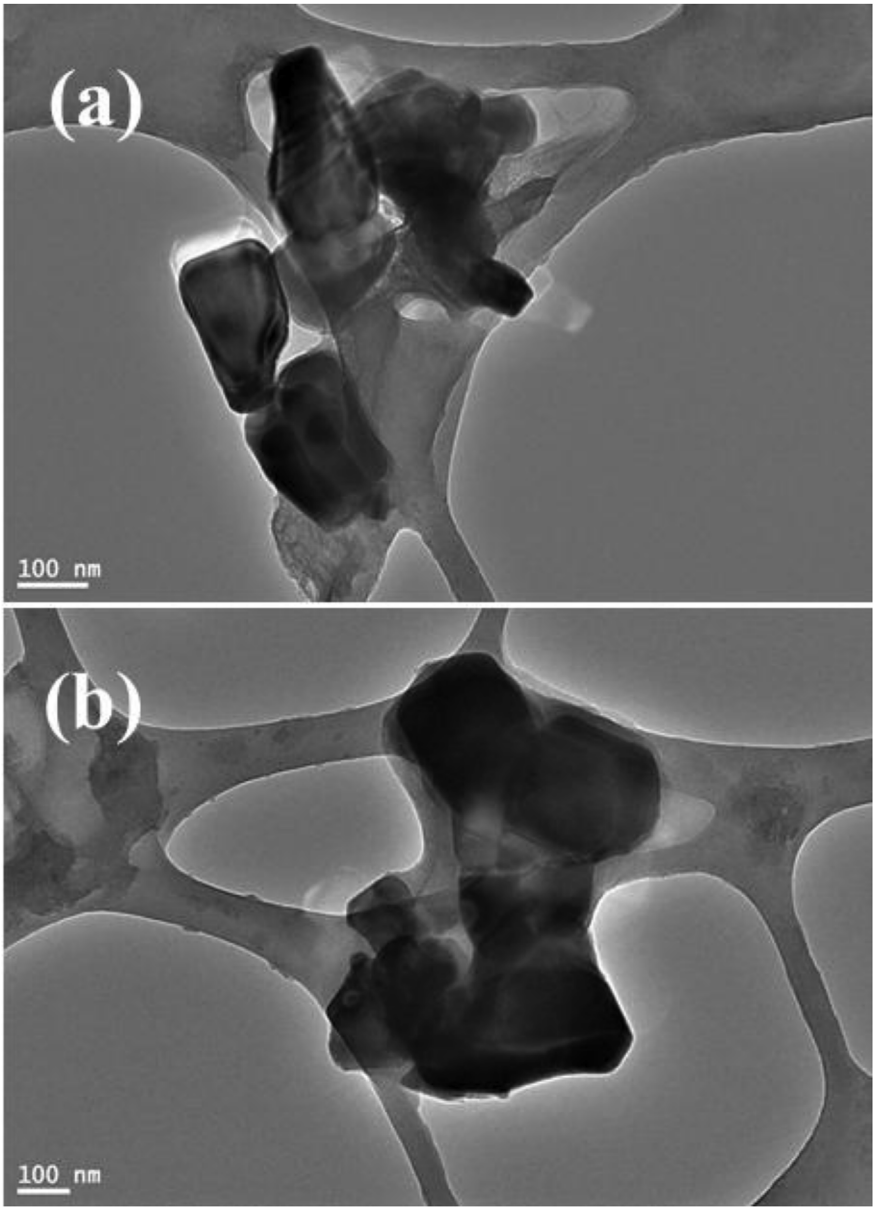

Fig. 2. The transmission electron microscopy (TEM) images of grown (a) and annealed at 250 °C of cubic shaped nanomagnesium oxide (CNMgO) (b).

~100–120 nm in range. The gaps between the particles were filled due to high temperature annealing process, and small particles are comes closer and form agglomerated cubic shaped magnesium oxide nanostructures. Due to annealing it forms the giant nanostructures, the average size of these cubic shaped nanostructures are ~150–200 nm (Fig. 2b).

3.3. FTIR spectroscopy

The white powder samples of as grown and annealed at 250 °C in air for 1 h were analyzed to check the functional change in the prepared material via the FTIR spectroscopy. The powder samples were mixed with KBr and form the pellets analyzed. In Fig. 3a the big and shallow peak position between 3429 cm^{-1} shows the asymmetric mode of vibration in hydroxyl group (O-H) [41,42], the annealing denotes the shifted position of shallow peak, which placed at 3439 cm^{-1} (Fig. 3b). The peaks at 2491 cm^{-1} denotes the CO_2 whereas the band at 1652-1630 cm^{-1} indicates the bending mode of vibration in water (HOH) molecule [41,42]. The long and sharp peak at 1451, 838-900 cm^{-1} defines symmetric and asymmetric stretching mode of vibration of nitro (NO_3^{2-}) group of used magnesium nitrate. The peak at 652 cm^{-1} (Fig. 3a) and 502 cm^{-1} (Fig. 3b) shows the metal/magnesium oxide peaks. These functional change states that the transformation of metal hydroxide into a metal oxide [41,42].

3.4. Thermogravimetric analysis (TGA) of CNMgO

Thermal changes accompanying in mass such as decomposition, sublimation, reduction, desorption, absorption, and vaporization can be measured by TGA [41]. The thermal decomposition of magnesium salts or alkoxides are found that the magnesium oxide can be obtained in the range of 350–400 °C with various particle morphologies. In Fig. 4a. It can be seen from sample the typical TGA weight loss shown on two regions. The first region, at 186 °C, corresponds to the solvent evaporation from bulk powder and at 502 °C shows the phase transition of magnesium hydroxide to magnesium oxide [41]. However in DTG (Derivative thermo-gravimetric) data of Fig. 4a. Shows a broad exothermic signal obtained around at 165 °C and at 455 °C a sharp

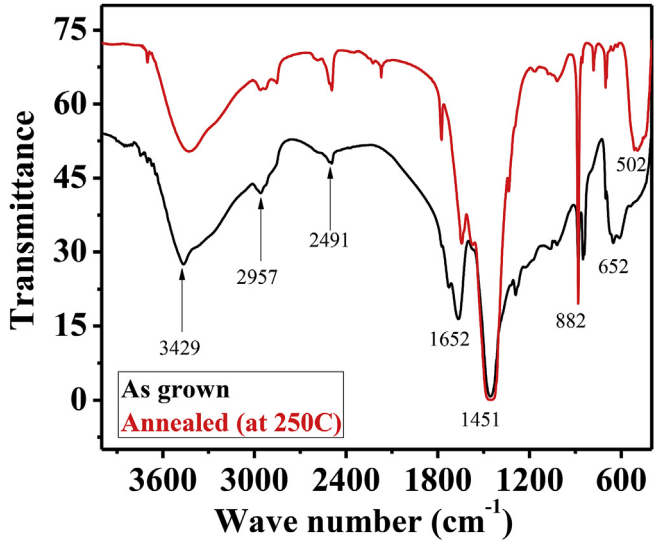

Fig. 3. FTIR spectroscopy of grown (a) and annealed (at 250 °C) cubic shaped nano magnesium oxide (CNMgO) (b).

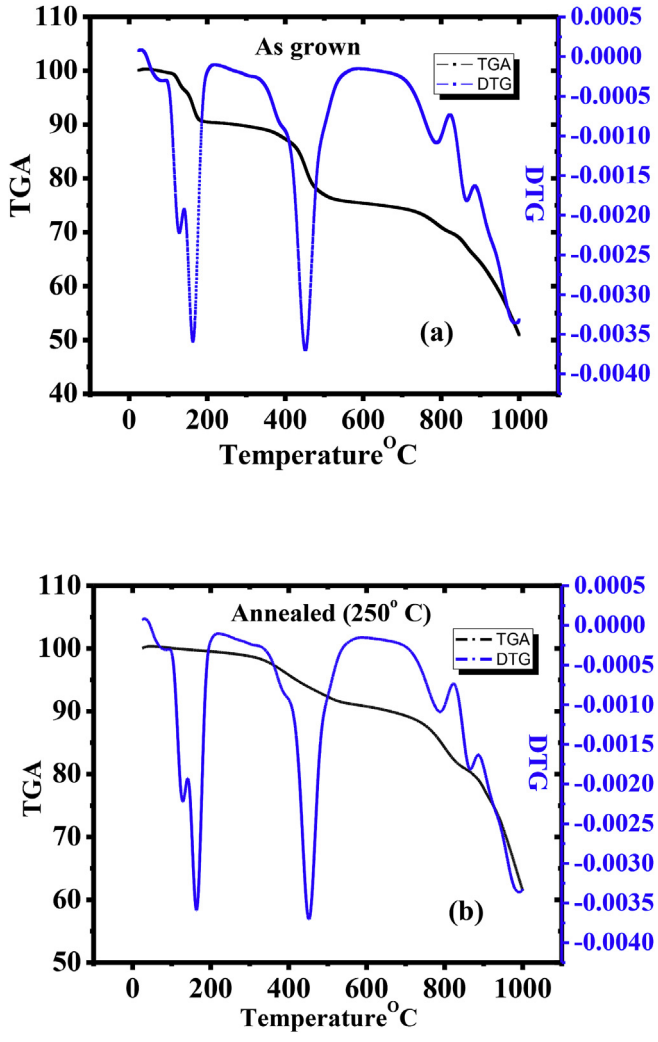

Fig. 4. TGA and DTG of as grown (a) and annealed (b) cubic shaped nano-magnesium oxide (CNMgO).

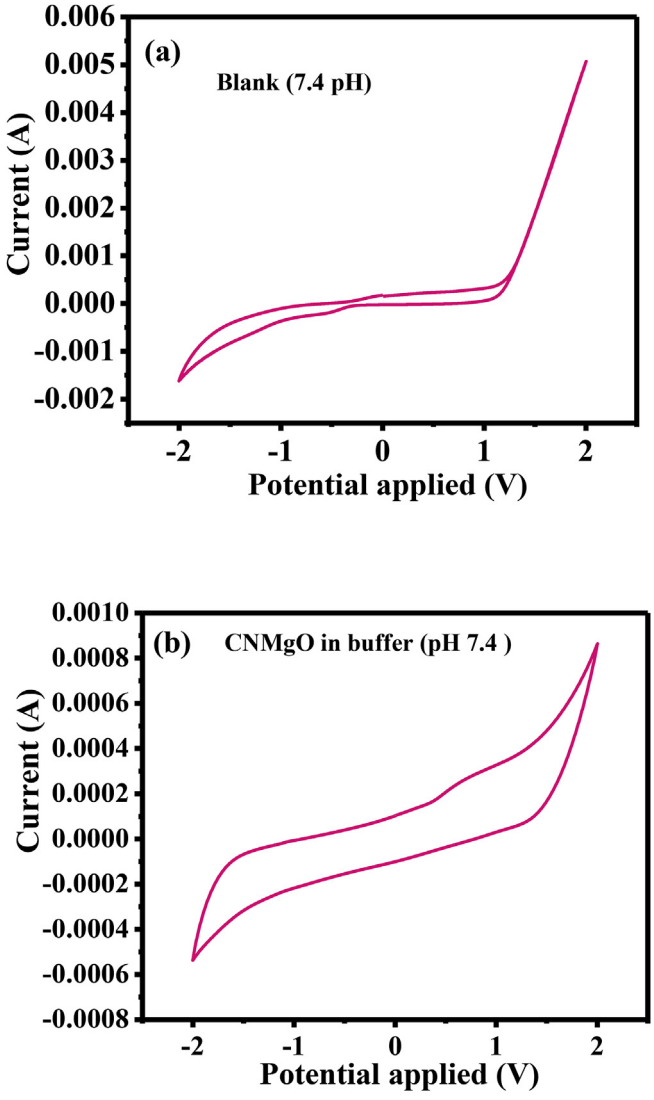

Fig. 5. Cyclic voltammetry curve of blank PBS (a) and cubic shaped nano-magnesium oxide (CNMgO) (b).

endothermic signal obtained which is close related to publish the data. It reveals phase transition of magnesium hydroxide in to magnesium oxide [41]. Fig. 4b Shows the annealed sample of magnesium oxide at 250 °C in air for 1 h. The TGA data show that there is flat curve is observed which is going to be setteled at higher temperatures. In this case there is no solvent evaporation peaks was observed. At ~550–600 °C shows the complete phase transition of CNMgO oxide [41]. In case of DTG data of Fig. 4b. Shows a small change in peak shift at 161 °C and at 448 °C which is due to the Exo and Endothermic signal change in the material.

3.5. Cyclic voltammetry (CV) results

The obtained CV curves for CNMgO samples with different concentration of hydrazine solution are shown here. To ascertain the material sensing characteristics, the prepared GCE electrode with CNMgO powder in hydrazine was used. The measurement was carried out at room temperature in presence of hydrazine solution at different concentration. Fig. 5a and b shows the CV graph in PBS buffer and MgO (Fig. 5b) respectively. It is observed that there is no oxidation and reduction peak has been observed in CV curve in absence of hydrazine however; a dramatic change in the CV curve was seen by the MgO nanostructures based electrode by the addition of low, mid and high

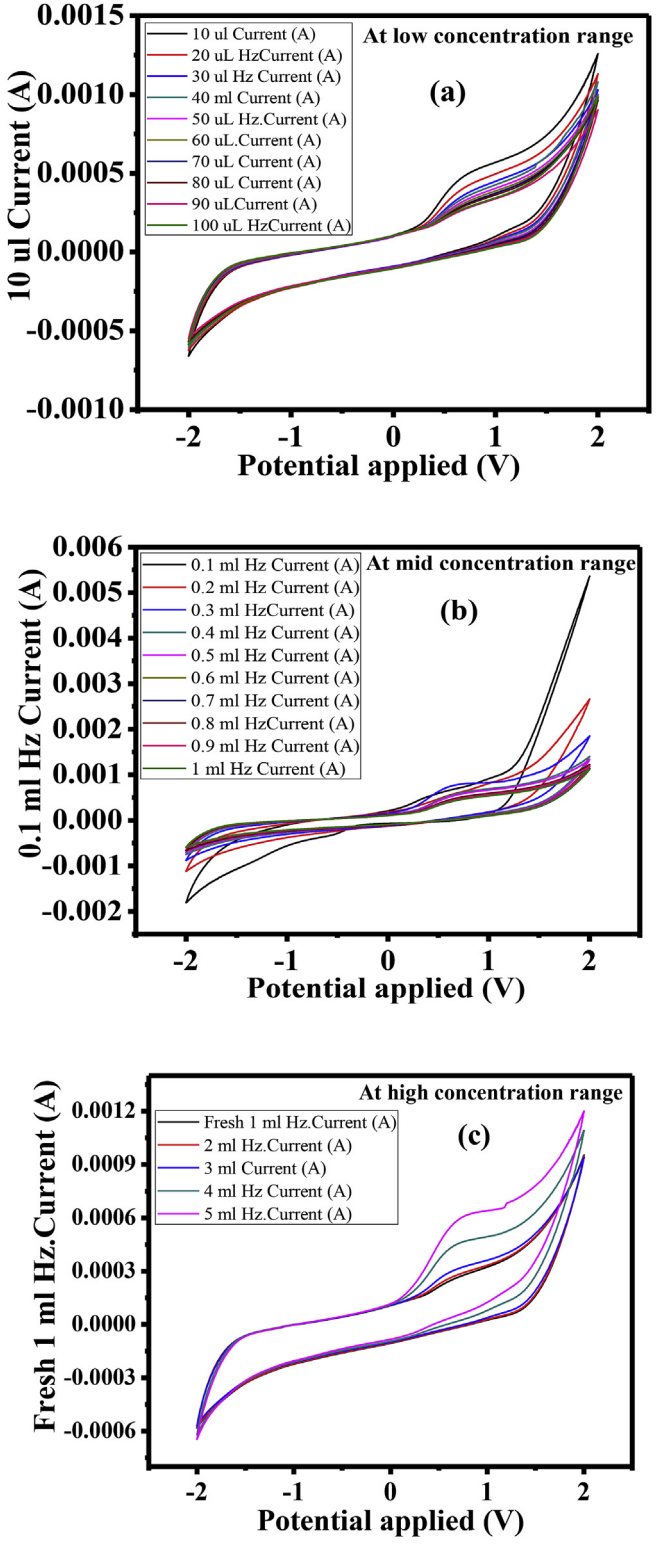

Fig. 6. Cyclic voltammetry curve of cubic shaped nanomagnesium (CNMgO) in presence of hydrazine solution: (a) at low (10, 20, 30, 40, 50,60, 70, 80, 90 and 100μL/100 μL buffer, (b) mid from 0.1, to 1 mL/100 mL PBS and (c) at high concentration from 1 mL to 5 mL/100 mL PBS (c).

concentration hydrazine at room temperature. Fig. 6a shows the CNMgONPs were covered with mixing at very low concentrations (10, 20, 30, 40, 50, 60, 70,80, 90,100 μL) of hydrazine (make up in 100 μL buffer) used. An increase in the electrical responses was noticed after addition of hydrazine as compared to electrical response measured in absence of hydrazine. The potential was cycled from −2.0 V to +2.0 V at a scan rate of 50 mV/S. To understand, charge transfer properties, scan rate variation was studied. The systematic changes was observed, which shows that the hydrazine has a potential electrical signals, represent the sensing responses in presence of NPs, which may be due to the good electron exchange properties of MgO nanomaterials. It is also observed that at higher concentration of hydrazine from 0.1, to 1 mL/100 mL PBS (Fig. 6b), a systematic curve related to the oxidation potential was observed which again confirm the electron displacement analyzed. As the doses/concentration of hydrazine increases to their enhanced condition (1 mL–5 mL/100 mL PBS (Fig. 6c)), there is not much difference was observed in the oxidation peak at 1–3 mL of hydrazine in 100 mL solution, whereas at 4 and 5 mL of hydrazine in 100 mL solution shows the oxidation potential with the influence of CNMgO. In this condition, we may postulate that at high concentration of hydrazine (4 and 5 mL) solution, which has the plenty of hydrogen molecules and can be easily, reacts with the CNMgONPs. The hydrazine has the property to liberate hydrogen and can possible to couple with the surface of the CNMgONPs. The obtained signal in the CV curve is the clear indication of liberation and interaction of hydrogen molecule from the hydrazine and reaction with NPs.

3.6. Possible mechanism

The hydrazine (N_2H_4), which is an industrial material and has wide application in various field such as storage, explosives fuel cells, propellants, pharmaceuticals, rocket prope llants etc. Over the wide range of application of the material it can cause skin and respiratory problems due to the carcinogenic and hepatotoxic nature in their substances. So it is an urgent demand to develop a highly sensitive and selective process for the detection of traces of hydrazine sensor [43,44]. The prepared CNMgO plays an important role to enhance the electroactive properties due to their large number of active sites and higher surface properties provides the larger detection of electrochemical detection of hydrazine at low (10, 20, 30, 40, 50, 60, 70,80, 90,100 μL), mid (0.1, to 1 mL/100 mL PBS) and high (1 mL–5 mL/100 mL PBS) concentrations. In our experiment we found that, at low concentration of hydrazine works electrochemical sensing properties whereas not much change were observed in mid-range concentration of hydrazine. When the concentration of hydrazine was increases in buffer solution, sudden change were observed in the oxidative and reduced peaks position, which is may be the higher number of ions enhance the electrochemical properties of hydrazine. The GCE of CNMgO emerges as an active material for the electrochemical sensing of hydrazine. The present work is the primary phase, which is useful to detect and develop the practical approach for hydrazine sensing for the large application in industries and environmental studies. The schematic shows (Fig. 7a) the experimental detail of electrochemical studies of prepared GCE on CNMgO electrode with hydrazine in PBS solution and was analyzed with the autolab potentiostat (Fig. 7b), collected the data's and analyzed (Fig. 7c and d). As per the previous studies [45-46] the metal oxide that has sensing surfaces due to the chemisorbed properties. In this, at initial the atmospheric oxygen molecules are physisorbed on the surface sites and it moves from site to site and gets ionized by extracting an electron from the conduction band and is thus ionosorbed on the surface as O^-_{ads} (O^- or O^{2-} depending on the energy available). This leads to a decrease in the conductance of sensor, as indicated by an increase in potential barrier at the grain boundaries. The resulting equation is;

$$O_2 + 2e^- \; 2O^-_{ads} \quad (1)$$

The reaction occur on this surfaces, immobilized samples and this is rate determining step and it affect the response time of the sensor. The performance of the sensor can be further enhanced by the use of proper catalyst, where the catalyst may help in further splitting the molecule and then it spill over on the whole surface of the prepared electrode/

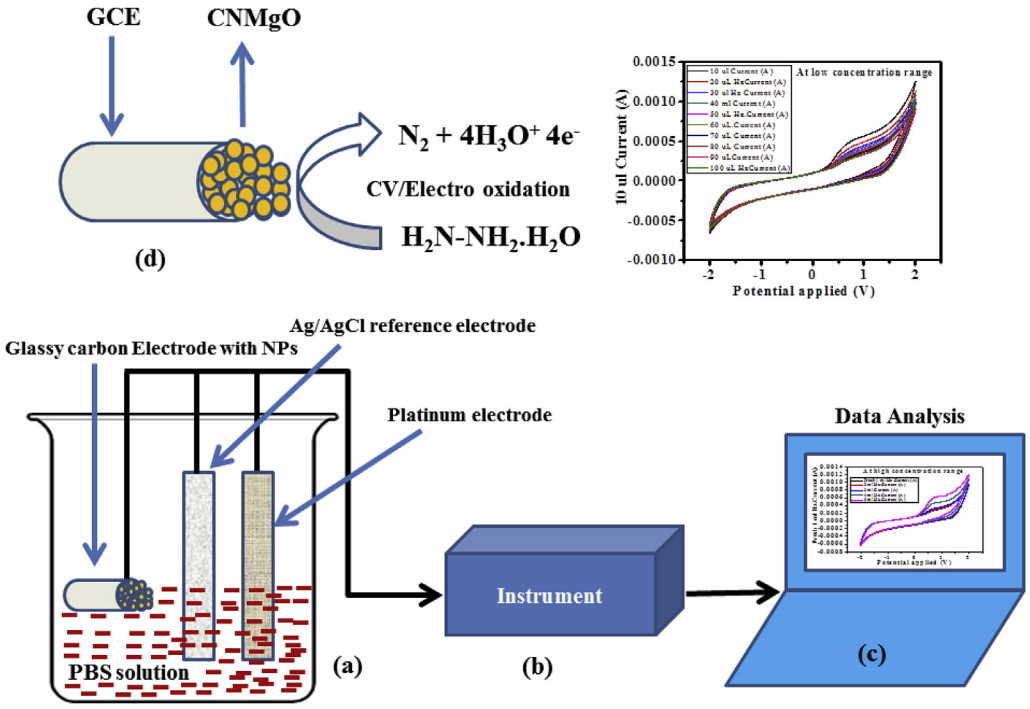

Fig. 7. Schematic showing the hydrazine sensing mechanism on GCE with CNMgO and their experimental set up.

template. This will enhance the reaction with pre-adsorbed surface oxygen of host material thereby increasing the conductance further and enhancing the response [45-46].

4. Conclusion

The work summarized here, have successfully synthesized the cubic shaped nanomagnesium oxide nanoparticles via solution process with using magnesium nitrate and sodium hydroxide. The prepared cubic shaped nanoparticles were well characterized with the instruments such as the X-ray diffraction pattern (XRD) were employed to know the crystalline property of the material, whereas the morphology of the material was examined with transmission electron microscopy (TEM). The functional behavior of the material was also evaluated via FTIR spectroscopy. The phase transition of the material was analyzed via the TGA heated from room temperature to 800 °C, which represents the stability of the grown and annealed nano structured material. The Derivative thermo-gravimetric (DTG) data showed that the exothermic and endothermic signal confirms that conversion of phase transition of metal oxides. The oxidation and reduction potential was analyzed via the cyclic voltammetry at different concentration from low, mid and high range of hydrazine, which represents that the prepared cubic shaped nanomagnesium oxide nanoparticles exhibit the potential to enhance the electrochemical properties and are very useful to control and assessed hydrazine in the environment for the industrial applications.

Conflicts of interest

The authors declare that there are no conflicts of interest.

Acknowledgement

This project was supported by King Saud University, Deanship of Scientific Research, College of Sciences Research Center.

References

[1] S. Tsubakizaki, M. Takada, H. Gotou, K. Mawatari, N. Ishihara, R. Kai, Alternatives to hydrazine in water treatment at thermal power plants, Mitsubishi Heavy Ind. Tech. Rev. 46 (2) (2009) 43–47.
[2] X. Yan, F. Meng, Y. Xie, J. Liu, Y. Ding, Direct N_2H_4/H_2O_2 fuel cells powered by nanoporous gold leaves, Sci. Rep. 2 (2012) 941, http://dx.doi.org/10.1038/srep00941.
[3] R. Ahmad, N. Tripathy, Y.-B. Hahn, Highly sensitive hydrazine chemical sensor based on ZnO nanorods field-effect transistor, Chem. Commun. (J. Chem. Soc. Sect. D) 50 (2014) 1890.
[4] C. Zhang, H. Li, Z. Zhuo, R. Dugnani, C. Sun, Y. Chen, H. Liu, Facile fabrication of ultra-light and highly resilient PU/RGO foams for microwave absorption, RSC Adv. 7 (2017) 41321–41329.
[5] B.K. Chaudhary, J. Farrell, Preparation and characterization of Homo polymer polyacrylonitrile-based fibrous sorbents for arsenic removal, Environ. Eng. Sci. 31 (11) (2014) 593–601, http://dx.doi.org/10.1089/ees.2014.0169.
[6] M.A. Zharkova, G.I. Kudryavtsev, I.F. Khudoshev, T.A. Romanova, Thermo mechanical and chemical properties of cross-linked polyacrylonitrile fibres, Fibre Chem. 1 (2) (1969) 191–194.
[7] J.E. Troyan, Properties, production, and uses of hydrazine, Ind. Eng. Chem. (1953) 2608–2612.
[8] J. Zhang, H. Yang, G. Shen, P. Cheng, J. Zhang, S. Guo, Reduction of graphene oxide via L-ascorbic acid, Chem. Commun. (J. Chem. Soc. Sect. D) 46 (2010) 1112–1114.
[9] L. Savini, L. Chiasserini, A. Gaeta, C. Pellerano, Synthesis and anti-tube rcular evaluation of 4-quinolylhydrazones, Bioorg. Med. Chem. 10 (7) (2002) 2193–2198.
[10] K.M.J. Cheung, T.P. Matthews, K. James, M.G. Rowlands, K.J. Boxall, S.Y. Sharp, A. Maloney, S.M. Roe, C. Prodromou, L.H. Pearl, G.W. Aherne, E. McDonald, P. Workman, The identification, synthesis, protein crystal structure and *In vitro* biochemical evaluation of a new 3,4-diarylpyrazole class of Hsp90 inhibitors, Bioorg. Med. Chem. Lett 15 (14) (2005) 3338–3343.
[11] A.O.H. ElNezhawy, S.T. Gaballah, M.A.A. Radwan, Studying the reactivity of (phthalazin-1(2H)-on-2-yl) methyl trichloroacetimidate towards different C- and O-nucleophiles, Tetrahedron Lett 50 (48) (2009) 6646–6650.
[12] A. Patel, S. Bari, G. Talele, J. Patel, M. Sarangapani, Synthesis and antimicrobial activity of some new isatin derivatives, Iran. J. Pharm. Res. (IJPR) 5 (4) (2006) 249–254.
[13] D. Jin, X. Gu, X. Yu, G. Ding, H. Zhu, K. Yao, Hydrothermal synthesis and characterization of hexagonal $Mg(OH)_2$ nano-flake as a flame retardant, Mater Chem Phys 112 (3) (2008) 962–965.
[14] X. Gu, J.P. Camden, Surface-enhanced Raman spectroscopy-based approach for ultrasensitive and selective detection of hydrazine, Anal. Chem. 87 (2015) 6460.
[15] Health and Environmental Effects Profile for Hydrazine and Hydrazine Sulfate. U.S. Environmental Protection Agency, Washington, DC, EPA/600/X-84/332 (NTIS PB88161963).
[16] G.W. Watt, J.D. Chrisp, Spectrophotometric method for determination of hydrazine, Anal. Chem. 24 (12) (1952) 2006–2008.
[17] G.E. Collins, Gas-phase chemical sensing using electrochemiluminescence, Sensor. Actuator. B 35 (1–3) (1996) 202–206.

[18] C. Gojon, B. Dureault, N. Hovnanian, C. Guizard, A Comparison of Immobilization Sol-gel Methods for an Optical Chemical Hydrazine Sensor Sens & Actuators B 38, (1997), pp. 154–162.
[19] D.L. Ellis, M.R. Zakin, L.S. Bernstein, M.F. Rubner, Conductive polymer films as ultrasensitive chemical sensors for hydrazine and monomethyl hydra -zine vapor, Anal. Chem. 68 (5) (1996) 817–822.
[20] R. Ahmad, N. Tripathy, Y.B. Hahn, Highly sensitive hydrazine chemical sensor based on ZnO nanorods field-effect transistor, Chem. Commun. (J. Chem. Soc. Sect. D) 50 (2014) 1890.
[21] C. Kaittanis, S. Santra, J.M. Perez, Emerging nanotechnology-based strategies for the identification of microbial pathogenesis, Adv. Drug Deliv. Rev. 62 (2010) 408–423.
[22] M.U. Ahmed, M.M. Hossain, E. Tamiya, Electrochemical biosensors for medical and food applications, Electroanalysis 20 (2008) 616–626.
[23] I. Paulowicz, V. Postica, O. Lupan, N. Wolff, S. Shree, A. Cojocaru, M. Deng, Y.K. Mishra, I. Tiginyanu, L. Kienle, R. Adelung, Zinc oxide nanotetrapods with four different arm morphologies for versatile nanosensors, Sensor. Actuator. B Chem. 262 (2018) 425–435.
[24] O. Lupan, F. Schütt, V. Postica, D. Smazna, Y.K. Mishra, R. Adelung, Sci. Rep. 7 (2017) 14715.
[25] O. Lupan, N. Wolff, V. Postica, T. Braniste, I. Paulowicz, V. Hrkac, Y.K. Mishra, I. Tiginyanu, L. Kienle, R. Adelung, Ceram. Int. 44 (5) (2018) 4859–4867.
[26] M. Segev-Bar, H. Haick, Flexible sensors based on nanoparticles, ACS Nano 7 (10) (2013) 8366–8378.
[27] Z. Wang, S. Lee, K. Koo, K. Kim, Nanowire-based sensors for biological and medical applications, IEEE Trans Nanobiosci 15 (3) (2016) 186–199.
[28] M.M. Rahman, V.G. Alfonso, F.F. Santiago, J. Bisquert, A.M. Asiri, A.A. Alshehri, H.A. Albar, Hydrazine sensors development based on a glassy carbon electrode modified with a nanostructured TiO_2 films by electrochemical approach, Microchimica Acta 184 (7) (2017) 2123–2129.
[29] S. Purwajanti, L. Zhou, Y.A. Nor, J. Zhang, H. Zhang, X. Huang, C. Yu, Synthesis of magnesium oxide hierarchical microspheres: a dual-functional material for water remediation, ACS Appl. Mater. Interfaces 7 (38) (2015) 21278–21286.
[30] M.C.I. Homs, DNA sensors, Anal. Lett. 35 (2002) 1875–1894.
[31] C. Wagener, Molecular diagnostic, J. Mol. Med. (Berl.) 75 (1997) 728–744.
[32] F. Cheng, Z. Tao, J. Liang, J. Chen, Efficient hydrogen storage with the combination of lightweight Mg/MgH_2 and nanostructures, Chem. Commun. (J. Chem. Soc. Sect. D) 48 (2012) 7334–7343.
[33] Y.B. Hahn, R. Ahmad, N. Tripathy, Chemical and biological sensors based on metal oxide nanostructures, Chem. Commun. (J. Chem. Soc. Sect. D) 48 (2012) 10369–10385.
[34] P. Docampo, P. Tiwana, N. Sakai, H. Miura, L. Herz, T. Murakami, H.J. Snaith, Unraveling the function of an MgO interlayer in both electrolyte and solid-state SnO_2 based dye-sensitized solar cells, J. Phys. Chem. C 116 (430) (2012) 22840–22846.
[35] X. Mo, G. Fang, H. Long, S. Li, H. Wang, Z. Chen, H. Huang, W. Zeng, Y. Zhang, C. Pan, Unusual electroluminescence from n-ZnO@i-MgO core–shell nanowire color-tunable light-emitting diode at reverse bias, Phys. Chem. Chem. Phys. 16 (2014) 9302–9308.
[36] X. Zheng, L. Zhang, Photonic nanostructures for solar energy conversion, Energy Environ. Sci. 9 (2016) 2511–2532.
[37] K.M. Beck, A. G.Joly, W.P. Hess, Two-color laser desorption of nano structured MgO thin films, Appl. Surf. Sci. 255 (24) (2009) 9562–9565.
[38] B.O. Jung, D.C. Kim, B.H. Kong, D.W. Kim, H.K. Cho, Fully transparent vertically aligned ZnO nanostructure-based ultraviolet photodetectors with high responsivity, Sensor. Actuator. B Chem. 160 (1) (2011) 740–746.
[39] C.H. Kao, C.L. Chang, W.M. Su, Y.T. Chen, C.C. Lu, Y.S. Lee, C.H. Hong, C.Y. Lin, H. Chen, Magnesium oxide (MgO) pH-sensitive sensing membrane in electro lyte-insulator-semiconductor structures with CF4 plasma treatment, Sci. Rep. 7 (2017) 7185.
[40] Y.G. Zhang, H.Y. He, B.C. Pan, Structural features and electronic properties of MgO nanosheets and nanobelts, J. Phys. Chem. C 116 (43) (2012) 23130–23135.
[41] R. Wahab, S.G. Ansari, M.A. Dar, Y.S. Kim, H.S. Shin, Synthesis of magnesium oxide nanoparticles by sol-gel process, Mater. Sci. Forum 558 (2007) 983–986.
[42] P. Tamilselvi, A. Yelilarasi, M. Hema, R. Anbarasan, Synthesis of hierarchical structured MgO by sol-gel method, Nano Bulletin 2 (1) (2013) 30106.
[43] P.K. Kannan, S.A. Moshkalev, C.S. Rout, Electrochemical sensing of hydrazine using multilayer graphene nanobelts, RSC Adv. 6 (2016) 11329–11334.
[44] Y. Liu, S.S. Chen, A.J. Wang, J.J. Feng, X. Wu, X. Weng, An ultra-sensitive electro chemical sensor for hydrazine based on AuPd nanorod alloy nanochains, Electrochim. Acta 195 (2016) 68–76.
[45] R. Wahab, S.T. Khan, J. Ahmad, J. Musarrat, A.A. Al-Khedhairy, Functionalization of anti-*Brucella* antibody on ZnO-NPs and their deposition on aluminum sheet towards developing a sensor for the detection of *Brucella*, Vacuum 146 (2017) 592–598.
[46] R. Wahab, S.T. Khan, J. Ahmad, S.G. Ansari, J. Musarrat, A.A. Al-Khedhairy, MWCNTs functionalization and immobilization with anti-*Brucella* antibody; towards the development of a nanosensor, Vacuum 146 (2017) 623–632.